Engineering of antigen-saving dissolving microneedles for intradermal vaccine delivery

Lee, J.

CHAPTER 4

ENGINEERING OF AN AUTOMATED NANO-DROPLET DISPENSING SYSTEM FOR FABRICATION OF ANTIGEN-SAVING DISSOLVING MICRONEEDLE ARRAYS

Jihui Lee[1], Koen van der Maaden[2], Gerrit Gooris[1], Conor O'Mahony[3], Wim Jiskoot[1], Joke Bouwstra[1]

[1] Division of Biotherapeutics, Leiden Academic Centre for Drug Research, Leiden University, 2333CC Leiden, The Netherlands
[2] Department of Immunology, Leiden University Medical Center, 2300RC Leiden, The Netherlands
[3] Tyndall National Institute, Lee Maltings, Prospect Row, Cork, Ireland

Int. J. Pharm., (2021), DOI: 10.1016/j.ijpharm.2021.120473

ABSTRACT

The dissolving microneedle array (dMNA) is a promising device for intradermal vaccine delivery. The aim of this study was to develop a reproducible fabrication method for the dMNA based on an automated nano-droplet dispensing system that minimises antigen waste. First, a polymer formulation was selected to dispense sufficiently small droplets (<18 nL) that can enter the microneedle cavities (base diameter 330 μm). Besides, three linear stages were assembled to align the dispenser with the cavities, and a vacuum chamber was designed to fill the cavities with dispensed droplets without entrapped air. Lastly, the dispenser and stages were incorporated to build a fully automated system. To examine the function of dMNAs as a vaccine carrier, ovalbumin was loaded in dMNAs by dispensing a mixture of ovalbumin and polymer formulation, followed by quantifying the ovalbumin loading and release into the skin. The results demonstrate that functional dMNAs which can deliver antigen into the skin were successfully fabricated via the automatic fabrication system, and hardly any antigen waste was encountered. Compared to the method that centrifuges the mould, it resulted in a 98.5% volume reduction of antigen/polymer formulation and a day shorter production time. This system has potential for scale-up of manufacturing to an industrial scale.

GRAPHICAL ABSTRACT

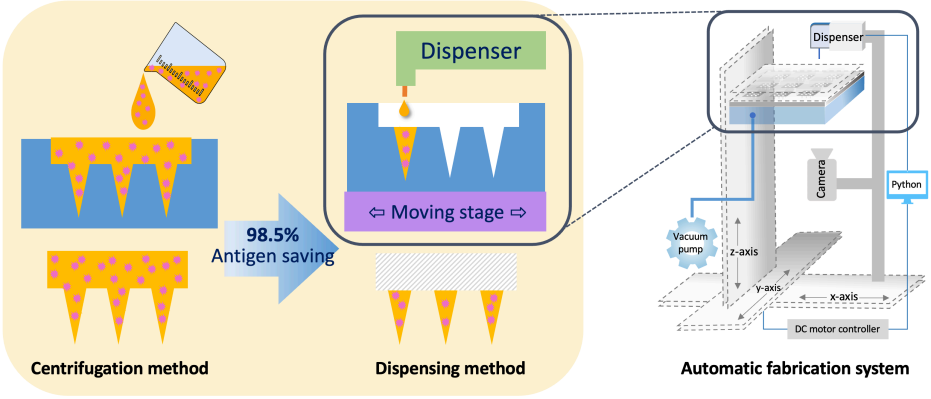

1. INTRODUCTION

Intradermal administration of antigens is attractive for vaccination because the skin is easily accessible and contains a large population of antigen-presenting cells[1,2]. Previous studies revealed that intradermal vaccination induces similar or higher levels of immune responses compared to subcutaneous or intramuscular administration. Intradermal vaccination against Aujeszky's disease induced higher levels of $CD8\beta^+$, $CD3^-CD8\alpha^+$, and $CD4^-CD25^+$ T lymphocytes compared to intramuscular administration[3]. Also, injection of muramyl dipeptide-loaded ovalbumin microspheres through the intradermal route showed relatively higher ovalbumin-specific IgG antibody immune response levels compared to the subcutaneous route[4].

However, the stratum corneum, the outermost layer of the skin, which acts as a barrier to protect the body from its environment, also prevents vaccines from entering the skin. To overcome this barrier, specialised delivery devices have been developed, such as tattooing, ballistic guns, ultrasound-based devices, and microneedles[5–8]. Among various intradermal delivery devices, one of the most attractive approaches is microneedles, because they deliver antigen and/or adjuvant intradermally, resulting in a sufficient immune response (*e.g.*, ovalbumin-specific IgG titers, $CD4^+$ and $CD8^+$ T-cells) in a minimally invasive manner[9]. Different types of microneedle technologies have been developed, including hollow, solid coated, solid with patch, porous, and dissolving. These microneedles are generally <1 mm in length.

So far, delivery of antigen using hollow[10,11], coated[12,13], porous[14], and dissolving[15] microneedles has shown to trigger efficient immune responses. Dissolving microneedles are of special interest because the antigen in a dissolving microneedle array (dMNA) is generally more stable compared to liquid dosage forms[16,17]. Therefore, a cold chain might be avoided. This is beneficial especially in low-income countries since high transport costs for the cold chain limit their vaccine coverage[14,18–21]. Moreover, compared to injectable lyophilised vaccine formulations, there is no need for reconstitution. dMNAs have additional advantages. For instance, there is no sharp-waste or risk of re-use since they dissolve in the skin upon administration. Furthermore, self-administration of dMNAs may be possible, which reduces the need for trained medical staff. This can accommodate the demand for increasing vaccination in developing countries by increasing the access to vaccination for people[22]. For these reasons, dMNAs are promising devices for intradermal vaccine delivery.

dMNAs can be made of sugars or biodegradable polymers, such as carboxymethylcellulose (CMC)[23], hyaluronic acid (HA)[24], and polyvinyl alcohol (PVA)[25]. In the past decade, dMNA production methods have shown considerable progress and diversity. The most common method uses centrifugation after casting the mixture of antigen and polymer into a mould[26,27].

Even though this concept is simple, the major drawback is huge antigen loss as the antigen is also present in the backplate of the dMNA, which is not inserted in the skin. Since the antigen is the most expensive part of the vaccine, antigen in the backplate leads to a huge loss of doses, which makes dissolving microneedle technologies less useful in pandemic situations.

To circumvent the antigen loss during the production of dMNAs, several methods have been investigated. The temperature and the viscosity of maltose solution were manipulated to produce dMNAs by drawing lithography[28] and multi-layers of different payload solutions were cast across the mould[29]. A piezoelectric dispenser also helped to load the antigen only in the microneedle tips[30].

In this study, we engineered a novel automated nano-droplet dispensing system for dMNA fabrication (automatic fabrication system). We demonstrated the step-by-step design from screening the most adequate polymer formulation, selecting a dispenser, building and integrating linear stages and designing a vacuum chamber, to filling a series of microneedle arrays. This novel automatic fabrication system resulted in a significant volume reduction (98.5%) of required polymer formulations compared to the centrifugation method. The mechanical stability and dissolution ability of fabricated dMNAs via the automatic fabrication system were investigated through ex vivo human skin penetration study and microneedle dissolution test. The potential use of dMNAs for vaccination purposes was evaluated by delivering the model antigen ovalbumin into ex vivo human skin and analysing the loaded and delivered amount of ovalbumin.

2. MATERIALS AND METHODS

2.1. Materials

SYLGARD 184 base silicone elastomer and curing agent silicone elastomer were purchased from Dow Corning (Midland, MI, USA). Polyvinylpyrrolidone (PVP, Mw 40 kDa), poly(ethylene glycol) (PEG, molecular weight 400 Da), PVA (Mw 9–10 kDa, 80% hydrolysed), CMC (low viscosity), gelatin and trypan blue solution 0.4% (w/v) were purchased from Millipore Sigma (Zwijndrecht, the Netherlands). Sodium hyaluronate (HA, average Mw 10 kDa, 20 kDa, and 100 kDa) was purchased from Lifecore Biomedical (Chaska, MN, USA). Vinylpolysiloxanes A-silicone (Elite Double 32) was from the Zhermack Group (Badia Polesine, Italy) and epoxy glue was from Bison International B.V. (Goes, the Netherlands). Tape (packing tape polypropylene, transparent) for stripping skin was purchased from Staples and ovalbumin-Alexa Fluor™ 647 conjugate was purchased from Thermo Fisher (the Netherlands).

Silicon microneedle arrays were kindly provided by Tyndall National Institute (Cork, Ireland). This silicon microneedle array has nine (3×3) of 500 µm long microneedles with a base

diameter of 330 µm on a backplate of 5×5 mm^2, and between each microneedle is a spacing of 1.75 mm. Three linear stages (two of M-403.4DG and one of M-403.2DG) were purchased from Physik Instrumente Benelux B.V. (the Netherlands) and a PipeJet® Nanodispenser was purchased from BioFluidix GmbH (Germany). A microscope camera (USB microscope 2 MP digital zoom) was purchased from Toolcraft. For SDS PAGE, sample buffer (#1610737), 4–20% Mini-PROTEAN TGX Precast protein gels (#4561094), Tris/glycine/SDS running buffer (#1610732), Coomassie Brilliant Blue R-250 staining solution (#1610436) were purchased from Bio-Rad (the Netherlands).

2.2. Polymer screening for the automatic fabrication system

2.2.1. Design of PMMA master structure and PDMS mould fabrication

dMNA fabrication started from a polymethylmethacrylate (PMMA) master structure which was made by the Fine Mechanical Department (FMD) at Leiden University. As shown in Figure 1, the PMMA master structure has nine pedestals (3x3) and the surface area of each pedestal is 5x5 mm^2. On top of each pedestal, a silicon microneedle array was attached. A polydimethylsiloxane (PDMS) mould was prepared from this PMMA master structure as previously described[27].

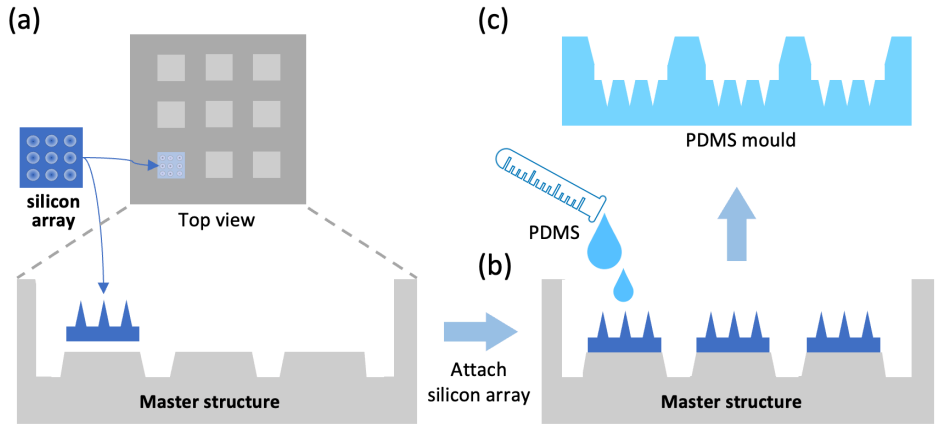

Figure 1. PDMS mould fabrication process. Nine silicon arrays were attached on the pedestals of a PMMA master structure (a). A PDMS mixture was poured into the master structure followed by overnight curing (b). The resulting PDMS mould has nine arrays and each array contains nine individual microneedles (c).

2.2.2. Fabrication of dMNAs using a centrifugation method

In order to screen the most suitable polymer formulation in terms of sharpness, penetration efficiency, dissolution rate, and viscosity to be used for the automatic fabrication system, first dMNAs were fabricated by using a modified centrifugation method which has previously

been developed in our group[27]. Among widely used biodegradable polymers for dMNAs fabrication, five different polymer candidates with various concentration and molecular weights were chosen for the polymer screening (Table S1): PVP/PEG, PVA, HA, CMC, and gelatin[23,31–33]. Solid polymer was added to 10 mM phosphate buffer (PB, pH 7.4, prepared with 7.7 mM Na2HPO4 and 2.3 mM NaH2PO4), and PEG was added only to PVP at a 5.6% (w/w) concentration to improve the rigidity and the flexibility of PVP-containing dMNAs[34,35]. The polymer in PB was shaken (IKA Vibrax VXR Basic, 1000 RPM) at 37 °C overnight to ensure homogeneous mixing. Only HA solutions were shaken at 4 °C because of their poor thermal stability[36].

The polymer concentration of each formulation was selected based on the ease of fabrication and the rigidity of produced dMNAs. Too high or too low polymer concentrations were excluded from further investigation and were defined as follows; Too high concentration resulted in too high viscosity to cast the formulation into a PDMS mould, and too low concentration produced too brittle dMNAs to handle. The highest viscosity that we cast to the mould was 429 mPa.s with 10% (w/v) HA 100 kDa, and the lowest viscosity was 6.64 mPa.s with 3.25% (w/v) PVP/PEG (17.8:1 weight ratio).

To fill the microneedle cavities of the PDMS mould, the polymer formulations were cast into the PDMS moulds and subsequently centrifuged (Beckman Coulter Allegra X12R Indianapolis, IN, USA) for 3 hours at 25 °C and 11,400 g. Only 40% (w/v) gelatine was centrifuged at 37 °C to facilitate the filling of microneedle cavities, as the viscosity was too high at low temperature. The centrifuged mould was incubated at 37 °C overnight for drying. The following day, silicone backplates were prepared from vinylpolysiloxane and epoxy glue and applied onto each array as previously reported[27]. The epoxy glue facilitates the demoulding of dMNAs from the PDMS mould. After removal, 3x3 dMNAs were cut into individual arrays and stored in a desiccator with silica-gel beads at room temperature (RT) until use. The shape and sharpness of the microneedles and the absence of air bubbles in the microneedles were investigated by using a brightfield microscope (Stemi 2000-C, Carl Zeiss Microscopy GmbH, Göttingen, Germany).

2.2.3. Skin penetration test in ex vivo human skin

The mechanical strength and sharpness of dMNAs fabricated via the centrifugation method were assessed by performing a skin penetration test. Human abdominal skin was collected from a local hospital after cosmetic surgery. Excess fat was removed, and the skin was stored at 80 °C until use. Prior to use, the skin was thawed at 37 °C for an hour, and subsequently stretched on parafilm-covered Styrofoam. To remove the sebum, the skin was cleaned by wiping it with 70% ethanol.

An impact-insertion applicator in conjunction with a microneedle applicator controller (uPRAX Microsolutions B.V., Delft, the Netherlands) was used to pierce the skin with a reproducible impact velocity (65 ± 1 cm/s)[37]. By using the applicator, a dMNA was applied on the skin and removed after one second. Next, 75 µL of 0.4% (w/v) trypan blue was dropped on the site of microneedle-treated skin. The trypan blue was removed from the skin after 45 min, and the stratum corneum was removed by around 10 times tape stripping in alternating directions. Finally, the skin was photographed and the number of blue spots, which indicate the number of penetrated microneedles, were analysed. The penetration studies for each dMNA formulation were carried out in quadruplicate. The penetration efficiency was calculated by dividing the number of penetrations (blue spots) by nine, the total number of microneedles in one array.

2.2.4. Microneedle dissolution test in ex vivo human skin

For vaccination, rapid dissolution of the microneedles (preferably <20 min) is desired to facilitate the application of dMNAs. To this end, we aimed to screen the polymer formulation that showed the fastest dissolution by displaying the shortest remaining height of microneedles after dissolution. Thereby, a microneedle dissolution test was executed and the remaining height of dissolved microneedles at the same time period was measured. dMNAs were applied onto the skin as described in Section 2.2.3, and the microneedles stayed in the skin for 5 min. The shape of the removed microneedle was visualised by using a brightfield microscope, and the remaining height of microneedles was measured. Three microneedles were tested for each formulation.

2.2.5. Viscosity

The next step after polymer screening via the skin penetration and microneedle dissolution tests was selecting the optimal polymer concentration to produce nano-droplets using the dispenser and fill the microneedle cavities of the mould. As the dispenser can only be used when the polymer formulations have a viscosity below 50 mPa.s, it is important to determine the viscosity of the polymer formulation. Therefore, the viscosity for various concentrations of the selected polymer was measured by using a viscometer (Brookfield Ametek, DV2T). The measurement was performed for 60 s at RT and 5 RPM in triplicate. The device was set at a shear rate and shear stress of 0.122 (1/s) and 0.04 (dyn/cm^2), respectively.

2.3. Automatic fabrication system

To reduce the loss of antigen-containing formulation, an automatic fabrication system was developed for loading it exclusively into the microneedle cavities. This system was composed of five main components: dispenser with its holder, vacuum chamber, microscope camera, linear stages, and a vacuum pump.

First, the dispenser (Figure 2a) was selected based on the size of droplets it can produce. To this end, a PipeJet® Nanodispenser was selected, which can generate droplets as small as 1.2 nL (132 µm of diameter) and thus fits easily to a single microneedle cavity (volume 14 nL, base diameter 330 µm). The dispenser was fixed on a 3D-printed dispenser holder (Figure 2b).

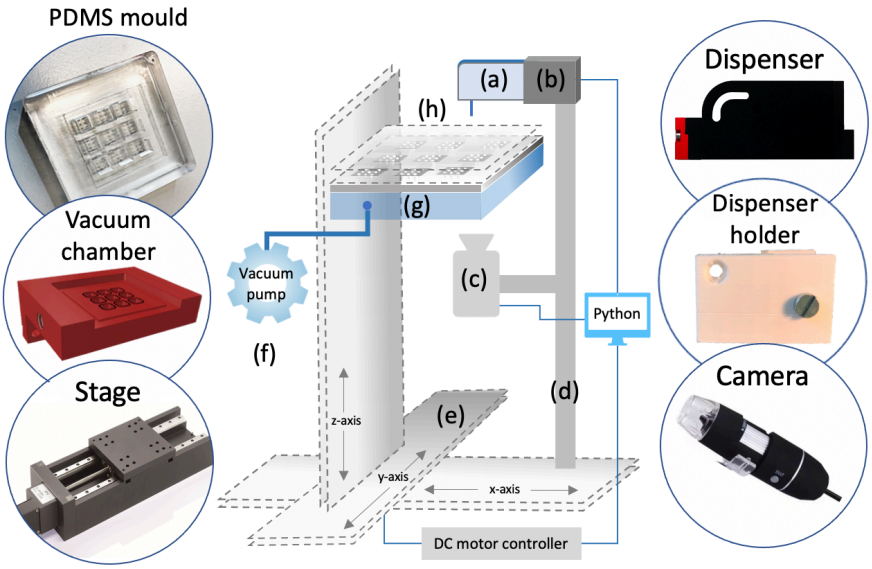

Figure 2. Schematic representation of the automatic fabrication system for dMNA fabrication. The automatic fabrication system consists of the following equipment; dispenser (a), dispenser holder (b), digital microscope camera (c), aluminium bar (d), linear stages (e), vacuum pump (f), and vacuum chamber (g). The PDMS mould (h) is placed on top of the vacuum chamber. Both the dispenser and the stages are operated by software, Python.

Next, a digital microscope camera (Figure 2c) was installed on the aluminium bar (Figure 2d) and positioned under the PDMS mould to visualise the filling of the microneedle cavities. Then, three linear stages (Figure 2e) were assembled to carry the PDMS mould in the x-, y-, and z-directions. On the z-stage, a vacuum chamber (Figure 2g) which was connected to a vacuum pump (Figure 2f) was fixed. This vacuum chamber was designed to support the PDMS mould (Figure 2h) and also remove the entrapped air in the microneedle cavities. Lastly, the dispenser and three linear stages were incorporated using software, Python (v3.8).

The process for dMNA fabrication via the automatic fabrication system is as follows. First, the PDMS mould is placed on the vacuum chamber and the vacuum pump is turned on. Three linear stages give movement to the PDMS mould, and the first microneedle cavity is aligned

with the dispenser nozzle. To confirm this alignment, the operation of dispenser and the movement of PDMS mould are calibrated and monitored by using the integrated microscope camera. Next, each microneedle cavity is sequentially filled with nano-droplets, while the reduced pressure is applied to the PDMS mould. Filling of the microneedle cavities is repeated until the desired volume has been loaded into the individual microneedle cavities of the PDMS mould. After filling of all nine microneedle arrays, epoxy glue is applied followed by overnight drying. The next day, dMNAs are carefully separated from the PDMS mould. The detailed set-ups of each component in the automatic fabrication system are described below.

2.3.1. Dispensing droplets into the microneedle cavities of the PDMS mould

As a result of the polymer formulations screening (see Section 3.1), 6.5% (w/v) PVP/PEG was selected to be used for the automatic fabrication system. In order to visualise the dispensing process clearly, 0.1% (w/v) rhodamine B dye was added to 6.5% (w/v) PVP/PEG. The dispenser was connected to a 1000 µL reservoir through 8–9 cm of a Teflon tube (inner diameter 1.6 mm, outer diameter 3.2 mm). Air bubbles in the tube were removed by tapping.

To optimise the dispensing process (before the dispenser holder and the vacuum chamber were designed), the dispenser was fixed by a ring stand and the mould was placed on the elevated flat surface. Each microneedle cavity was aligned with the dispenser nozzle manually by hand, and the dispensing process was monitored through the microscope camera.

2.3.2. Movement of linear stages

In order to position the microneedle cavities of the PDMS mould, the automatic fabrication system requires three linear stages: x-, y-, and z-stages (Figure 2e). Two long linear stages (M-403.4DG) were used for the x- and y-stages, and one short linear stage (M-403.2DG) was used for the z-stage. Each stage was connected to a direct-current gear motor controller and selected based on the accuracy of the motor's movement. The minimum incremental motion of the motor was 0.2 µm. Considering that the distance between each microneedle cavity was 1.75 mm, 0.2 µm was a high enough resolution to obtain an accurate alignment of each microneedle cavity with the dispenser nozzle.

The y-stage was installed perpendicularly to the x-stage, and the z-stage was installed on the y-stage perpendicularly to the x-y plane. Before incorporating the dispenser and stages using Python, the movement of stages to the desired position was controlled with its own software, PIMikroMove (v2.31.1.8). The PDMS mould can be moved between 0 and 100 cm for the x- and y-directions and between 0 and 50 cm for the z-direction.

2.3.3. Dispenser holder and microscope camera

To fix the dispenser at a predetermined position on the stage, a dispenser holder was designed by using SolidWorks (SOLIDWORKS Student Design Kit (2017–2018)) and 3D-printed (by FMD at Leiden University) with PMMA. Even a little movement of the dispenser can misalign the dispenser nozzle with the microneedle cavities. In order to prevent misalignment, the groove of the dispenser holder (Figure 2b) was designed in such a way that it can hold the dispenser tightly with a screw. Both the dispenser holder and the microscope camera (Figure 2c) were screwed on an aluminium bar (Figure 2d), which was installed on the x-stage. The microscope camera was controlled via MicroCapturePlus (v3.1).

2.3.4. Filling the microneedle cavities and design of the vacuum chamber

When air gets entrapped into the microneedle cavities, it hinders drawing down the polymer formulation to the tip, which results in diminishing the mechanical properties and sharpness of the microneedles. In order to avoid and/or remove air from the microneedle cavities, four different methods were assessed.

1) 0.01% (w/v) or 0.1% (w/v) polysorbate 80 (PS80) was added to 6.5% (w/v) PVP/PEG, the selected formulation, and dispensed into the microneedle cavities. The PS80 was expected to reduce the surface tension of the polymer solution and make it reach the tip. Dispensing was performed for seven cycles, and one cycle consists of filling all 81 microneedle cavities once.

2) A degassing step was added after each dispensing cycle. For degassing, the mould was placed in the vacuum vessel (100 mbar) for different time points: 30 sec, 2 min, 3 min, and 5 min. The vacuum was expected to drive out the air from the microneedle cavities.

3) The mould was centrifuged (11,400 g) after each dispensing cycle for 1 min, 2 min, and 5 min. The centrifugal force was supposed to remove the air by rising it up to the surface as it did during the fabrication via the original centrifugation method.

4) Reduced pressure was applied to PDMS moulds of two different thicknesses. As the PDMS mould is porous, the applied reduced pressure can suck the air from the microneedle cavities. In order to apply the reduced pressure to the bottom side of the PDMS mould, the mould was placed on the designed vacuum chamber (Figure 3), and each array of the PDMS mould could be placed on a square hole of the vacuum chamber. In this way, the reduced pressure could be applied directly to the microneedle cavities. The transparent vacuum chamber was fixed on the z-stage and positioned between the dispenser and the microscope camera (see Figure 2). Hence, the camera can monitor the dispensing process by imaging the PDMS mould.

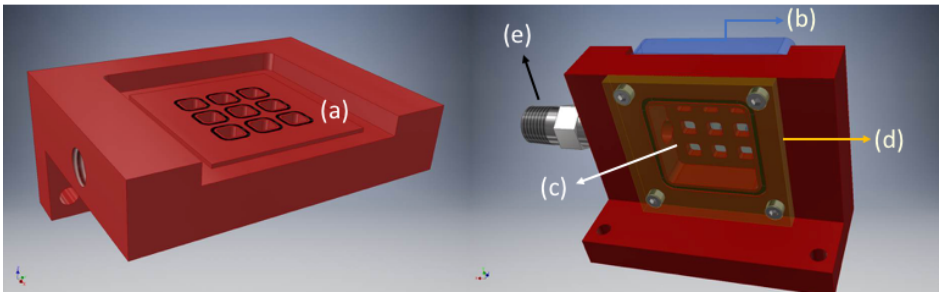

Figure 3. Design of the vacuum chamber. The PDMS mould is placed on the top of the vacuum chamber (a). The empty space under the PDMS mould (b) serves as the vacuum chamber (c). The top and bottom of the vacuum chamber are sealed with the PDMS mould and a transparent panel (d), respectively. The vacuum chamber is connected to the vacuum pump through the hose outlet (e).

The intensity of the reduced pressure and the thickness of the PDMS mould can affect the air removal efficiency in the microneedle cavities. In order to investigate the optimal conditions for removing the air, both the intensity of the reduced pressure and the thickness of the PDMS mould were varied, and the number of intact microneedles was counted after fabrication.

The thickness of the PDMS mould was either 8 mm or 4.5 mm (Figure 4), while three reduced pressures were applied: 100 mbar, 50 mbar, and 8 mbar. This allowed us to determine the minimum pressure needed to produce air-free microneedles. After the fabrication of dMNAs, the fraction of intact microneedles was calculated (n=3). For this, the number of intact microneedles was divided by 81 which was the total number of microneedles produced in one mould.

2.3.5. Automatic fabrication of dMNAs

To build a fully automated system, the dispenser and linear stages were incorporated and controlled by using Python. The filling process starts from lifting up the PDMS mould using the z-stage, so that the array can reach the dispenser nozzle as close as possible. The x- and y-stages can shift their positions from 0 to 100 cm, and each microneedle cavity is aligned with the dispenser nozzle by designating the position of the microneedle cavity through the software. For example, if we want to move the PDMS mould to the middle of each stage, we need to input its desired position as (50, 50). The position of the first microneedle cavity is set as (a, b) and the position of the additional 80 microneedle cavities is allocated by adding the distance (x, y) from the first microneedle cavity to the microneedle cavity of interest (a + x, b + y).

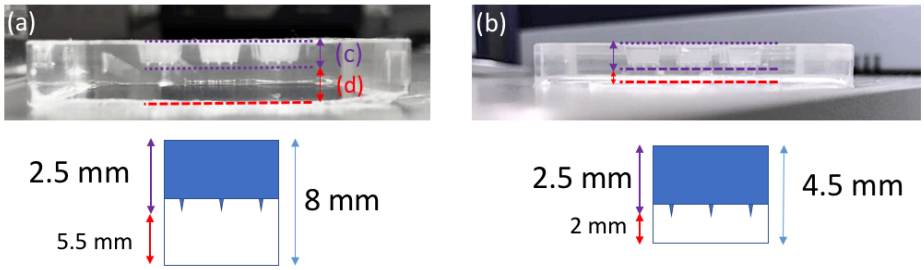

Figure 4. PDMS moulds with 8 mm (a) and 4.5 mm (b) thickness. In both designs, the length from the upper surface of the mould to the tip of the microneedles (c, purple) is always equal to 2.5 mm. Therefore, the thickness of moulds is decided by the length from the tip of the microneedles to the bottom surface of the mould (d, red).

Based on the results of dispenser optimisation (Section 3.2.1), the droplet size was set to 1.5 nL. After alignment, 10 shots of a 1.5 nL droplet entered the first microneedle cavity. Then, the x-, y-stages shift the PDMS mould again and align the next microneedle cavity with the dispenser. In order to determine the minimum number of dispensing cycles for air-free microneedles, the number of cycles was varied from 5 to 10. After dispensing process, epoxy glue was applied on dMNAs followed by drying, and dMNAs were carefully removed as described in Section 2.2.2.

2.3.6. Analysis of the integrity of automatically fabricated dMNAs

The shape of the automatically fabricated dMNAs was analysed by using a brightfield microscope. In order to monitor that the microneedles were completely filled without any air bubbles, we also visualised the cross-section of microneedles using a scanning electron microscope (SEM, Nova NanoSEM-200, FEI, Hillsboro, OR, USA). The microneedle was cut at 360 µm height from the base by using a microtome (Leica RM2235, Germany) and the SEM was set at an acceleration voltage of 2 kV, a working distance of 10.1 mm, and a current of 13 pA. Furthermore, the distribution of polymer with rhodamine B dye in the dMNA was visualised by using a fluorescence microscope (Zeiss Imager D2, camera AxioCam MRm, light source HXP120V, Carl Zeiss MicroscopyGmbH, G¨ottingen, Germany).

2.4. Automatic fabrication of ovalbumin loaded dMNAs

In order to demonstrate the function of dMNAs as an antigen carrier, AF647 labelled ovalbumin (AF647-ovalbumin) was loaded in dMNAs as a model antigen. As ovalbumin increased the viscosity, the total concentration of PVP/PEG together with ovalbumin was decreased from 6.5% (w/v) to 5% (w/v) to lower the viscosity and increase the dissolution rate. The ratios between PVP/PEG and ovalbumin were varied, while keeping the total

concentration the same: 4:1 (4% (w/v) PVP/PEG and 1% (w/v) ovalbumin) and 1:1 (2.5% (w/v) PVP/PEG and 2.5% (w/v) ovalbumin). After the mixture was shaken overnight at 4 °C, dMNAs were fabricated as described in Section 2.3.5 with 10 dispensing cycles. The skin penetration and microneedle dissolution tests were carried out as described in Sections 2.2.3 and 2.2.4, respectively. The penetrated skin and residual microneedles after dissolution were analysed by using brightfield and fluorescence microscopes.

2.5. Loading efficiency and released amount of ovalbumin

To determine the loading efficiency of ovalbumin in the dMNA, AF647-ovalbumin loaded dMNAs (n=3) were added to 300 µL PB and shaken overnight at 4 °C. On the next day, the fluorescence intensity of the dMNAs dissolved PB and the same volume (1.35 µL) of dispensing solutions (AF647-ovalbumin and PVP/PEG mixture, n=3) was measured by using a Tecan Infinite M1000 plate reader (Männedorf Switzerland) with an excitation wavelength of 650 nm and an emission wavelength of 668 nm. The loading efficiency was calculated as a ratio of fluorescence intensity of AF647-ovalbumin in dMNAs and in dispensing solutions.

To determine the delivered amount of AF647-ovalbumin from dMNAs to the skin, the dMNAs before and after dissolution were added to 300 µL PB (n=3) and shaken overnight at 4 °C. The fluorescence intensity of AF647-ovalbumin in both solutions was determined. To determine the amount of ovalbumin dissolved, the fluorescent intensity value after dissolution of the dMNAs was subtracted from that of the dMNAs before the dissolution test.

2.6. Sodium dodecyl sulphate polyacrylamide gel electrophoresis (SDS-PAGE)

The stability of ovalbumin in the dMNA was characterised with SDS-PAGE. The ovalbumin loaded dMNA was added to 300 µL of PB and shaken overnight at 4 °C. Then a sample was prepared by mixing 25 µL of dMNA dissolved PB with an equal volume of sample buffer (65.8 mM Tris-HCl pH 6.8, 26.3% (w/v) glycerol, 2.1% SDS, 0.01% bromophenol blue, 5% (v/v) β-mercaptoethanol). This mixture was loaded into a 4–20% polyacrylamide gel. Electrophoresis was performed in Tris/glycine/SDS running buffer under constant voltage at 150 V for 60 min. The gel was stained by using Coomassie Brilliant Blue R-250 staining solution for 15 min and destained in water:methanol:acetic acid solution (50:40:10 v/v/v) for an hour. Quantification of stained protein bands was performed by using a calibrated densitometer (Bio-Rad GS-800, the Netherlands) and bands were analysed with Image Lab (v 6.1).

2.7. Statistical analysis

The remaining height of dissolved microneedles was analysed by using one-way ANOVA. The level of significance was set at $p < 0.01$.

3. RESULTS

3.1. Centrifugation-based fabrication method and selection of polymer formulation

3.1.1. dMNA fabrication using the centrifugation method

dMNAs were successfully fabricated using the centrifugation method with five different polymers and various concentrations, as listed in Table S1. The microscopic images showed that each microneedle had a symmetrical conical shape with a sharp tip (Figures 5a and 5b). Some polymer formulations were discarded based on difficulties during the fabrication process or improper mechanical strength after fabrication. On the one hand, too low concentrated polymer solutions (*e.g.*, 3.25% (w/v) PVP/PEG) resulted in too brittle dMNAs (Figure 5c) to carry out the skin penetration test. On the other hand, too high polymer concentrations (*e.g.*, 50% (w/v) PVA) resulted in too viscous solutions to cast onto the mould. Therefore, 3.25% (w/v) PVP/PEG, 10% (w/v) 5 kDa HA, 50% (w/v) PVA, and 30% (w/v) CMC solutions were excluded.

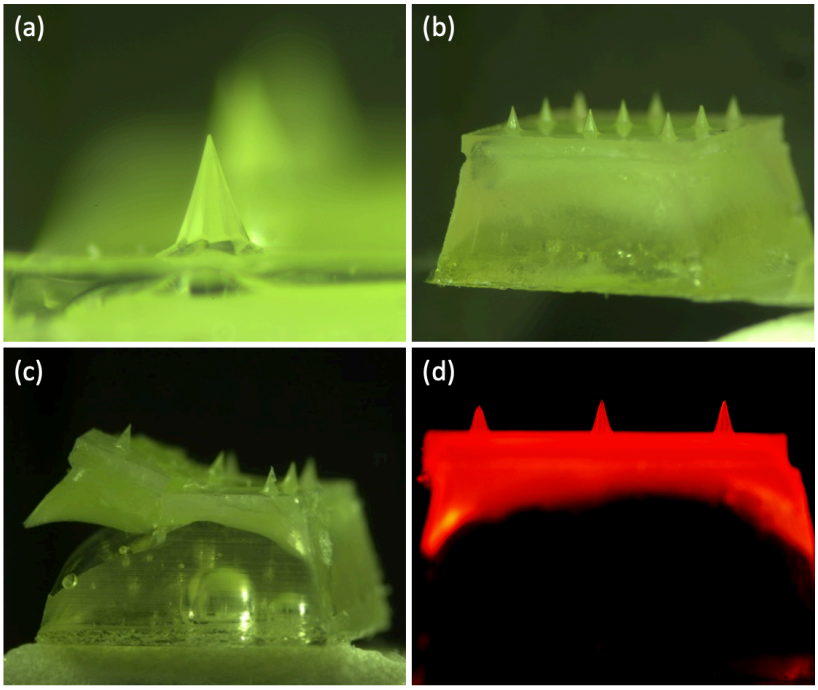

Figure 5. Fabricated dMNAs by using the centrifugation method. Brightfield microscopic images of representative examples of polymer formulations that resulted in sharp and strong conical dMNAs made of 6.5% (w/v) PVP/PEG (a) 10% (w/v) PVA and (b). Brittle dMNA made of 3.25% (w/v) PVP/PEG (c). Fluorescence microscopic image of 6.5% (w/v) PVP/PEG (d).

With all polymer formulations (except those excluded with too high/low polymer concentrations, as defined in Section 2.2.2), dMNAs were fabricated and used for further studies. In the fluorescence microscopic image of the fabricated dMNA (Figure 5d), the red part in the array indicates that PVP/PEG with a fluorescent dye (rhodamine B) is spread over the array.

3.1.2. Skin penetration test in ex vivo human skin

To determine whether the selected dMNAs (fabricated via the centrifugation method) can penetrate the skin, a skin penetration study was performed. The studies showed that all selected dMNAs displayed excellent penetration efficiencies in human abdominal skin (Figure S1 and Table 1). In total 9 out of 15 dMNAs from the various polymer formulations displayed 100% penetration efficiency (n=4). The lowest penetration efficiency (91.7%) was shown for 40% (w/v) gelatine dMNAs, indicating that at least 8 out of 9 microneedles in one array could penetrate the skin.

Table 1. List of polymer formulations and penetration efficiency of dMNAs. The selection of polymer formulations was based on their viscosity during the fabrication process and the mechanical properties (*i.e.*, rigidity) of dMNAs after fabrication. The discarded polymer formulations are listed in Table S1. The data was presented as mean ± SD (n=4).

Polymer concentration (% (w/v))	Penetration efficiency (%)						
	PVP/PEG	PVA	HA 10 kDa	HA 20 kDa	HA 100 kDa	Gelatin	CMC
5		91.7 ± 5.6					
6.5	100 ± 0.0						
10		100 ± 0.0	97.2 ± 5.6	97.2 ± 5.6	97.2 ± 5.6		100 ± 0.0
13	100 ± 0.0						
20		100 ± 0.0					100 ± 0.0
26	100 ± 0.0						
30		100 ± 0.0					
40		100 ± 0.0				91.7 ± 5.6	
52	97.2 ± 5.6						

3.1.3. Microneedle dissolution test in ex vivo human skin

Since fabricated dMNAs from each polymer formulation demonstrated sufficient mechanical strength and over 90% penetration efficiency in the skin penetration test, the next step of screening the polymer formulation was based on a microneedle dissolution test. Residual microneedles after 5 min dissolution were analysed by using a brightfield microscope (Figure S2). From the microscopic image, the leftover height of microneedles from each formulation was measured and provided in Figure 6. Among all microneedles, microneedles prepared with 6.5% (w/v) PVP/PEG showed the shortest average remaining height as 43.8 µm (8.8% of

full height). In contrast, microneedles prepared from 40% (w/v) gelatin hardly dissolved and showed the tallest residual height as 334.9 µm (67.0% of full height). In general, the graph clearly shows that the residual height of the microneedles decreased together with the molecular weights or concentration within the same kind of polymer. Based on the results of the microneedle dissolution test, PVP/PEG was selected for further studies.

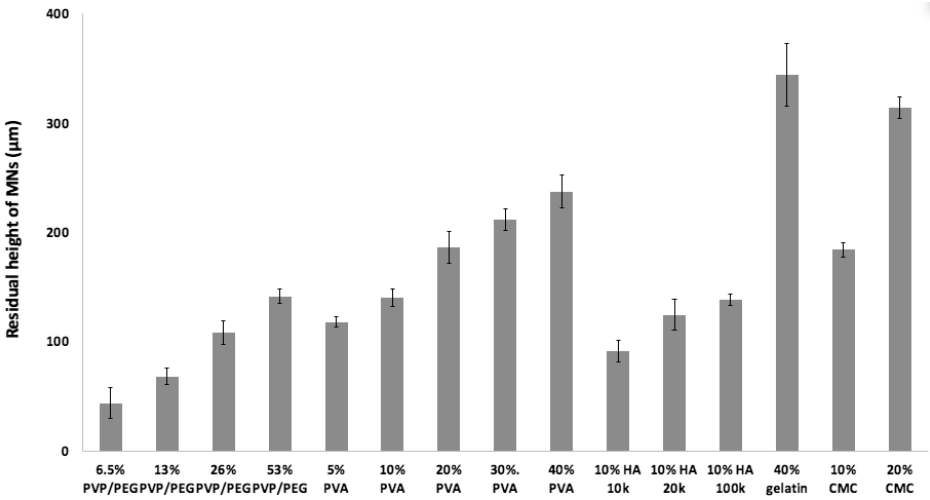

Figure 6. Residual height of microneedles after 5 min dissolution time in ex vivo human skin. The higher bar shows more residual height and subsequently more remaining volume of microneedles in the same time period (n=3, three microneedles measured once, Error bars=SD).

3.1.4. Viscosity

As the dispenser can handle formulations with a viscosity up to 50 mPa.s, the viscosity of 6.5–52% (w/v) PVP/PEG formulations were measured in order to select the proper concentrations of PVP/PEG to be used in the dispenser. With increasing the concentration of PVP/PEG, the viscosity also increased from 7.8 mPa.s to 96.2 mPa.s (Figure 7). From this, it is clear that concentrations ranging from 6.5% (w/v) to 26% (w/v) were adequate for the dispenser, while the 52% (w/v) PVP/PEG solution was out of the working range. Since a lower polymer concentration showed a faster dissolution (see Section 3.1.3), a PVP/PEG concentration of 6.5% (w/v) was selected for the development of an automatic fabrication system.

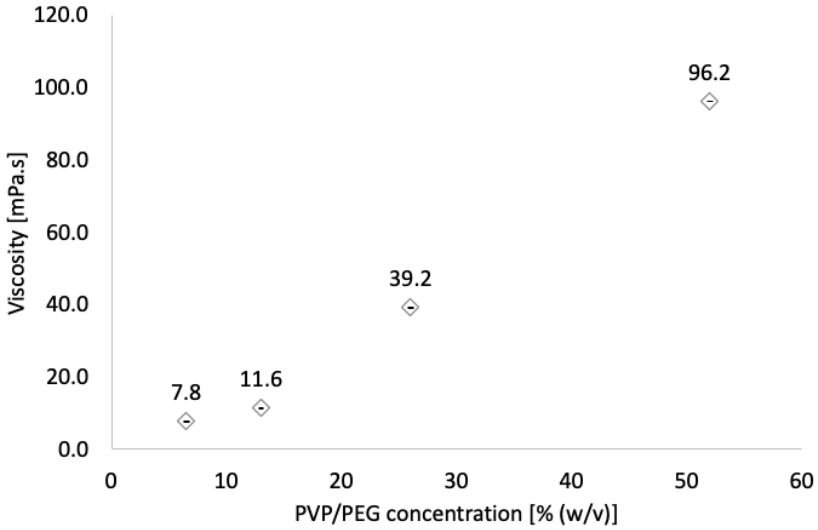

Figure 7. The viscosity of PVP/PEG formulations. The viscosity of PVP/PEG polymer formulation increases as the concentration of the polymer increases. The viscosity was measured by using a viscometer at RT and 5 RPM (Brookfield Ametek DV2T, USA). Error bars represent standard deviations. (n=3, triplicate preparations measured once)

3.2. Automatic fabrication of dMNAs

3.2.1. Optimisation of nano-dispenser

Prior to dispensing droplets with the selected polymer solution, optimisation of the nano-dispenser was required. According to the specifications of the dispenser, the smallest droplet volume that the dispenser can produce is 1.2 nL (diameter 132 µm). As the entrance diameter of the microneedle cavities is 330 µm, assuming that the droplets are spherical, droplets with a volume of up to 18.8 nL can enter the microneedle cavities (base diameter 330 µm). However, we observed that smaller droplets allowed better tip filling, whereas larger droplets easily got stuck at the tip entrance and resulted in a loss of polymer solution. Therefore, it was decided to dispense 10 shots of 1.5 nL droplets at a frequency of 10 Hz to fill each microneedle cavity.

After dispensing 10 droplets, the water in dispensed polymer solution evaporated and the microneedle cavity created space for the next dispensing cycle, while the dispenser filled the other 80 microneedle cavities. Sequential dispensing of 10 drops into all 81 cavities of 9 microneedle arrays is referred to as one dispensing cycle. As the number of dispensing cycles increased, the cumulative amount of polymer in the microneedle cavities also increased (Figures 8a to 8c). After seven cycles, the microneedle cavities were filled and no more polymer solution could be dispensed, since the entrance of the cavities was blocked (Figure

8c). As no automatic moving system was introduced yet, these studies were made by manual displacement of the PDMS mould.

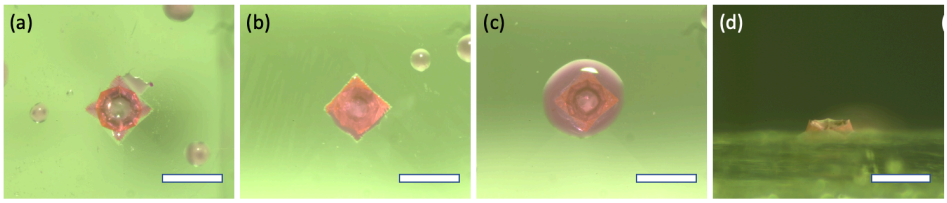

Figure 8. Dispensed nano-droplets into the microneedle cavities and removed microneedle after dispensing. Brightfield microscopic images of microneedle cavities after the first (a), fifth (b), and seventh cycles (c). The absence of a microneedle tip (d) indicated the presence of air in the microneedle cavities (scale bar = 300 µm).

As a result of filling, the dispensed droplets of seven cycles failed to display a sharp tip (Figure 8d), and it suggested the entrapment of air in the microneedle cavities. Possibly, the hydrophilic-hydrophobic interface between the polymer solution and the PDMS mould created this air. Therefore, the filling of the microneedle cavities needed to be improved to avoid air entrapment in the microneedle cavities.

3.2.2. Filling the microneedle cavities

In order to prevent and/or remove the air in the microneedle cavities, four different methods were investigated.

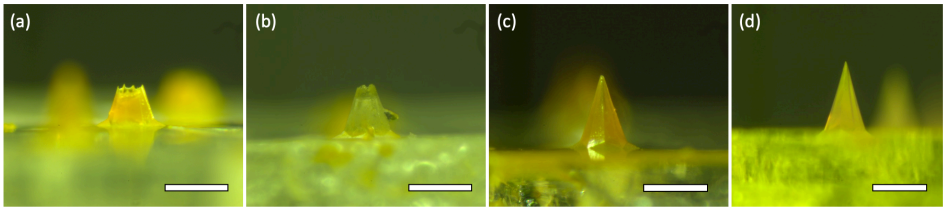

Figure 9. Fabricated 6.5% (w/v) PVP/PEG microneedles by using four different methods to fill the microneedle cavities completely. Adding 0.1% (w/v) PS80 (a) and performing a degassing step for 5 min after each dispensing cycle (b) drew down the solution closer to the tip of the microneedles. The centrifugation step for 5 min (c) was sufficient to fabricate a sharp microneedle without air. Applying reduced pressure during the dispensing cycles (d) also successfully removed the air in the microneedle. (scale bar = 300 µm)

1) A concentration of 0.01% (w/v) or 0.1% (w/v) PS80 was added to 6.5% (w/v) PVP/PEG to lower the surface tension of the solution. However, adding PS80 to the polymer solution did not result in sharp tips of the microneedles, even at a PS80 concentration of 0.1% (Figure 9a).

2) After each dispensing cycle, microneedle arrays were moved to a vacuum vessel for degassing at 100 mbar. The degassing step drew down the polymer solution closer to the tip and extended the height of microneedles, however, it failed to fill the microneedle cavities completely even after degassing for 5 min (Figure 9b).

3) A centrifugation step was performed after each dispensing cycle. This method showed better tip formation compared to the previous two methods. However, even though the polymer formulation reached the tip of the microneedles after 2 min of centrifugation, air bubbles were still trapped in the microneedles. To remove these air bubbles, a longer centrifugation time of 5 min was required (Figure 9c). Compared to the initial centrifugation method, adding a centrifugation step after each dispensing cycle reduced the centrifugation time from 3 hours to 5 min. However, it requires seven centrifugation steps, because the dispensing cycles were executed seven times. Besides, it cannot construct a fully automated system as it demands moving the mould from the automatic system to the centrifuge after each dispensing cycle.

4) Reduced pressure was applied to PDMS moulds of different thicknesses during the dispensing process. Three different reduced pressures of 100 mbar, 50 mbar, and 8 mbar were applied to PDMS moulds with a thickness of 8 mm and 4.5 mm (see Figure 4). The reduced pressure was delivered to the microneedle cavities through a specially designed vacuum chamber (Section 2.3.4).

When the same pressure was applied, more intact microneedles were observed with the 4.5 mm thickness mould compared to the 8 mm thickness mould (Table 2). Figure 9d shows that 8 mbar with 4.5 mm thickness of PDMS mould was sufficiently strong so that the entrapped air was removed from the microneedle cavities. In conclusion, applying reduced pressure via the vacuum chamber was the most successful method among the four different approaches for air removal from the microneedle cavities. For further experiments, 8 mbar of pressure and 4.5 mm thickness of PDMS mould were used.

Microneedles were also analysed individually by SEM after cutting them with a microtome in order to confirm that there was no air bubble entrapped. The appearance of the cross-sections in the images confirmed that no air bubbles were entrapped in the fabricated microneedles (Figures 10a and 10b). Next, the operations of the dispenser and stages were successfully incorporated using Python. Dispensing droplets and positioning of the PDMS mould were alternately repeated until completing the designated number of cycles.

Table 2. Percentage of intact microneedles as a function of PDMS mould thickness and reduced pressure. When pressure and PDMS mould thickness decreased, the number of intact microneedles increased. (n=3, triplicate preparations measured once)

Vacuum pressure	8 mm PDMS	4.5 mm PDMS
100 mbar	35.4% intact microneedles (SD = 4.33%)	75.3% intact microneedles (SD = 1.23%)
50 mbar	56.4% intact microneedles (SD = 0.71%)	90.1% intact microneedles (SD = 1.23%)
8 mbar	70.0% intact microneedles (SD = 1.43%)	97.1% intact microneedles (SD = 0.71%)

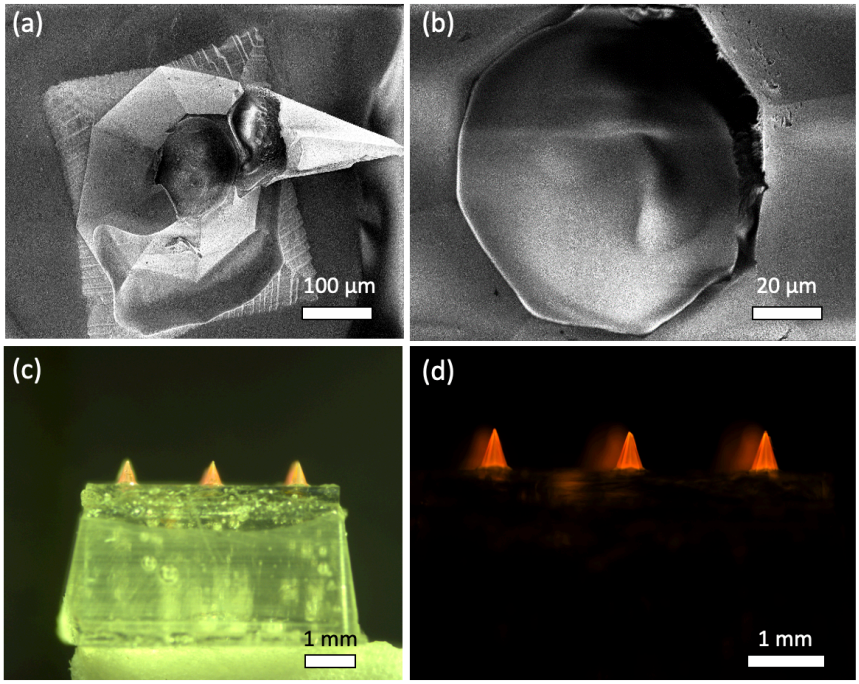

Figure 10. Representative microscopic images of 6.5% (w/v) PVP/PEG dMNAs fabricated with 8 mbar of vacuum and 4.5 mm of PDMS thickness. To ensure air-free microneedles, microneedles were cut horizontally, and their cross-sections were imaged by SEM (a and b). Rhodamine B dye was added to the 5% (w/v) PVP/PEG solution and its distribution in dMNAs was analysed by using brightfield (c) and fluorescence (d) microscopes. Both images illustrate that the polymer formulation with rhodamine B dye is exclusively present in the microneedles.

3.3. Comparison of fabricated dMNAs by the centrifugation method and the automatic fabrication system

After automatically fabricating dMNAs, the distribution of polymer formulation was compared to centrifugally prepared dMNAs. For the automatically fabricated dMNA, the fluorescent dye, which was added to the polymer solution, was located only in the microneedles (Figures 10c and 10d). In contrast, the fluorescent dye spread over the array including the backplate for the dMNA fabricated via the centrifugation method (Figure 5d). This indicates that substantially less antigen-containing formulation is needed for the dispensed method compared to the centrifuged method. As the automatic fabrication required 10 dispensing cycles to fill the microneedle cavities completely, it demanded only 1.35 µL (1.5 nL x 10 droplets x 10 cycles x 9 MNs) of 6.5% PVP/PEG solution to fabricate one dMNA by the dispensing method, while the centrifugation method required 90 µL of minimum volume.

In the skin penetration and microneedle dissolution tests, the automatically fabricated dMNAs showed similar results to dMNAs fabricated via the centrifugation method with 100 ± 0% penetration efficiency and 58.1 µm (11.6% of full height) of remaining height within 5 min of dissolution (data not shown).

3.4. Ovalbumin loaded dMNAs and delivery into the skin

In order to demonstrate that antigens can be incorporated in the automatically fabricated dMNAs while maintaining the dMNA properties, fluorescent dye AF647-ovalbumin was loaded in dMNAs as a model antigen. AF647-ovalbumin loaded in dMNAs with a 4:1 ratio of PVP/PEG:AF647-ovalbumin resulted in a sharp microneedle shape, as shown in Figure 11a.

AF647-ovalbumin loaded dMNAs showed 100 ± 0% penetration efficiency (n=4, Figure 11b), and the fluorescence in the penetrated skin indicated that AF647-ovalbumin in the microneedle was successfully delivered into the skin (Figure 11c). For the dissolution test (n=3), the remaining height of dissolved microneedles was 199.4 ± 23.3 µm (39.9% of full height) and 66.8 ± 2.4 µm (13.4% of full height) after 5 min (Figure 11d) and 15 min (Figure 11e and 11f) dissolution, respectively (Table 3). Compared to the empty dMNAs (without ovalbumin), which showed 43.8 µm (8.8% of full height, fabricated via centrifugation method) and 58.1 µm (11.6% of full height, fabricated via the automatic system) of residual height after 5 min dissolution, AF647-ovalbumin containing dMNAs displayed slower dissolution.

Based on the protein concentration (10 mg/mL) and the total volume dispensed into the microneedle cavities (1.35 µL), the dispensing solution contained 13.5 µg of ovalbumin.

Based on the fluorescence intensity of AF647-ovalbumin loaded dMNAs, 13.3 ± 0.15 µg of ovalbumin was loaded in the dMNA, which corresponds to a loading efficiency of 98.7 ± 1.11% of AF647-ovalbumin. After dissolving the microneedles, the remaining amount of AF647-ovalbumin in dMNAs was 4.73 ± 0.09 µg. Therefore, 8.57 µg (13.3 – 4.73 µg) of AF647-ovalbumin was delivered into the skin. After characterising ovalbumin in dMNA with SDS-PAGE, a single band corresponding to ovalbumin was observed at 45 kDa without signals of aggregation or fragmentation (data not shown).

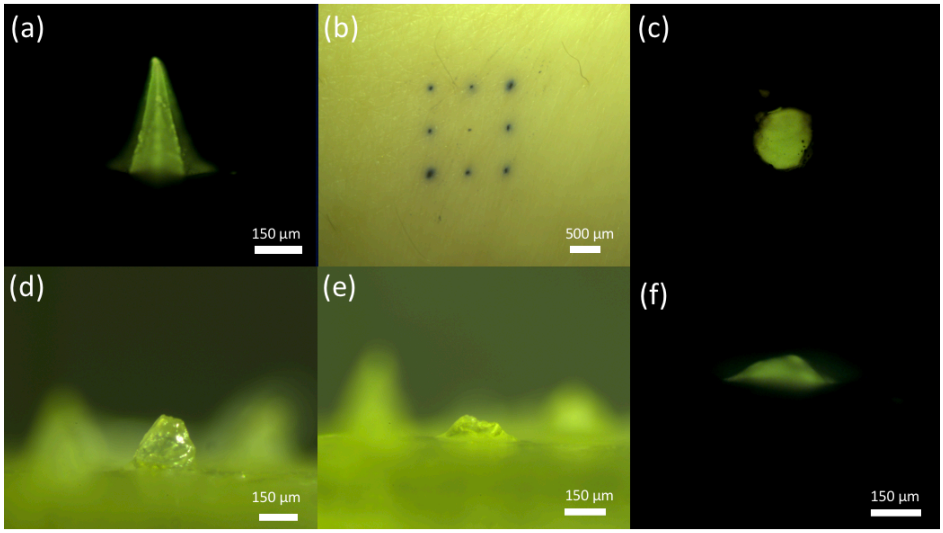

Figure 11. Microscopic images of AF647-ovalbumin loaded microneedles. A microneedle containing AF647-ovalbumin before skin penetration (a). 100% skin penetration efficiency (b, n=4) indicates its sharpness and mechanical strength. Successful delivery of ovalbumin is revealed from the fluorescence in the penetrated skin (c). Brightfield microscopic images of leftover microneedles after 5 min (d) and 15 min (e) dissolution. Fluorescence microscopic image of the remained microneedle after 15 min dissolution (f).

Table 3. Skin penetration efficiency and remaining height of empty and AF647-ovalbumin loaded microneedles. AF647-ovalbumin loaded dMNAs displayed the same penetration efficiency compared to empty dMNAs. The height of AF647-ovalbumin loaded microneedles after 15 min dissolution was higher than that of empty microneedles after 5 min dissolution, but there was no significant difference ($p > 0.01$). The data was presented as mean ± SD (n=4 for penetration efficiency and n=3 for dissolution test).

	Empty dMNAs	**AF647-ovalbumin loaded dMNAs**
Penetration efficiency (%)	100 ± 0	100 ± 0
Remaining height after 5 min dissolution (µm)	43.8 ± 13.9	199.4 ± 23.3
Remaining height after 15 min dissolution (µm)	N/A	66.8 ± 2.4

4. DISCUSSION

In this study, an automatic dMNA fabrication system was engineered, and its design procedure was illustrated step by step from the selection of a dispenser to the incorporation of stages and the dispenser. Our aim was to develop a method to minimise the antigen waste and shorten the fabrication time compared to a commonly used centrifugation method. Eventually, the automatic fabrication system successfully replaced the centrifugation method with decreased required volume of (antigen-containing) polymer formulation and reduced fabrication time.

Despite its ease of application, the centrifugation method has a critical drawback, especially for the scale-up fabrication, which is a high antigen loss. In order to solve this problem, various approaches have been developed to date. One of them is loading the drug solution only into the microneedle tip by removing the excess solution in the base part with a spatula[38]. Another method is the 3D-printing technique that avoids the presence of antigen in the base part by building up a pyramid with a cone shape of microneedles on the substrate followed by washing with isopropyl alcohol to remove excess resin[39]. The spraying technique also reduces antigen waste and produce multi-layer dMNAs[40]. Two different formulations are applied by spraying an antigen-containing formulation and a backplate formulation. All these techniques for dMNA fabrication resulted in a reduction of polymer formulation or/and antigen waste. Nevertheless, they still required an additional fabrication step such as removal of excess antigen solution and applying an additional layer of the formulation. The spray technique also couldn't avoid the loss of antigen as it sprayed not only into the cavities of the microneedle tip but also at the surface of the microneedle mould.

To minimise the antigen waste using a single step fabrication method, we developed a precise dispensing method with a nano-droplet dispenser and an accurate positioning of the PDMS mould. In terms of using the dispenser and stages, our automatic fabrication system has similar aspects, as compared to the system described by Allen *et al*.[30]. However, a major difference in our approach is that we applied reduced pressure instead of mould wetting in order to remove entrapped air in the microneedle cavities. Therefore, preparing an additional formulation for wetting the mould is not necessary and fabrication time can be further decreased as the reduced pressure is applied during the dispensing process. Further differences are the size of droplets and the covered viscosity range. Their Piezo dispensing technology can produce smaller droplets as 1-70 pL, however, the viscosity range of polymer formulations is lower (<20 mPa.s) than our system (<50 mPa.s). This viscosity issue can narrow down the number of dispensable polymer formulations. Therefore, the optimal ratios between PVA/trehalose/tween were selected considering viscosity below 20 mPa.s. Their dispenser and stages were incorporated using LabVIEW which can facilitate the system

operation for users as it displays an eidetic view of the system and demands a simple operation compared to coding. Their extended study[41] also shows successful skin penetration and delivery of formulation in the human skin with empty dMNAs (without antigen).

As a result, the automatic fabrication system overcame the limitations of prior arts by dispensing antigen solution only into the microneedle tip. Numerically, the automatic fabrication system showed antigen loading efficiencies close to 98.7%, while the conventional process showed loading efficiencies of about 0.14%. Consequently, this can lead to a dramatic reduction in the preparation cost of antigen loaded dMNAs. In addition to the economic advantage, this method can easily be scaled up, as the dispensing process is executed automatically by programming, which makes it attractive for low-cost manufacturing at an industrial scale.

Using the current settings with a concentration of 10 mg/mL ovalbumin and a 1.35 µL dispensing volume, we could deliver 8.57 µg of ovalbumin into the skin. In a previous study, a dose as little as 0.4 µg of ovalbumin induced similar level of IgG titers compared to 15 µg of ovalbumin administration through intramuscular route[29]. Therefore, we consider the loaded and released amount of ovalbumin sufficiently high to induce an immune response.

To establish a fully automated production process, there are some parts of the automatic fabrication system that may be improved. Firstly, it is envisaged to develop an optical detection system. The shape of the microneedle mould needs to be adjusted, depending on the dosage of antigen and the desired radius of the microneedle base[42]. As a different design of moulds requires a different code for the alignment of the dispenser with respect to the microneedle cavities, developing an optical sensor for detection of microneedle cavities can facilitate the alignment without re-writing the code[41].

Secondly, engineering an additional step for automatic demoulding of dMNAs is advantageous. The combination of 8 mbar of pressure and 4.5 mm of mould thickness resulted in 97% of intact microneedles. The damaged 3% microneedles were mostly from the edge of the mould, and the damage mainly occurred during the removal of dMNAs from the mould as other studies also reported[38,43]. This is because the demoulding step is the most delicate part of the whole fabrication process, and the microneedles are not precisely vertically removed from the mould. Hence, automatic demoulding of dMNAs can lower the number of damaged microneedles by applying a vertical ejecting force[44] to dMNAs alongside holding the PDMS mould with a sucking or pulling force to the other side.

Lastly, multiple nozzles of the dispenser are necessary to speed up the fabrication, especially for industrial-scale fabrication. This not only reduces fabrication time but also enables the loading of numerous drug formulations into a single dMNA. Therefore, we can extend this study to design multilayer dMNAs. By optimising the viscosity and/or concentration of each polymer/antigen formulation and layering them into the microneedle cavities, the release of each polymer/antigen formulation is controllable as desired[45,46].

In order to perform additional quality control of dMNAs, more stability tests of dMNAs are required. For example, storage of dMNAs at different humidity and temperature conditions[47], followed by a skin penetration test can be executed. Also, mechanical forces can be applied to dMNAs to determine the fracture force[48].

In conclusion, we have engineered an automated system for dMNA fabrication. The selected polymer formulation, 6.5% (w/v) PVP/PEG, with or without antigen, met two critical requirements for the resulting dMNAs: sufficient mechanical strength which can penetrate the skin and rapid dissolution upon administration (<15 min). Moreover, using the automatic dMNA fabrication system minimises antigen loss and reduces production time, opening the possibility of low cost industrial-scale production.

ACKNOWLEDGEMENTS

We thank Gert Koning (FMD at Leiden University) for his generous support for the equipment setup. This work was supported by the Netherlands Organisation for Scientific Research (NWO, TTW15240). Koen van der Maaden is the recipient of a H2020-MSCA-Intra European Fellowship-2018 (Grant Number 832455).

REFERENCES

1. Engelke, L., Winter, G., Hook, S. & Engert, J. Recent insights into cutaneous immunization: How to vaccinate via the skin. *Vaccine* **33**, 4663–4674 (2015).
2. Skobe, M. & Detmar, M. Structure, function, and molecular control of the skin lymphatic system. *Journal of Investigative Dermatology Symposium Proceedings* **5**, 14–19 (2000).
3. Ferrari, L. *et al.* Evaluation of the immune response induced by intradermal vaccination by using a needle-less system in comparison with the intramuscular route in conventional pigs. *Res Vet Sci* **90**, 64–71 (2011).
4. Puri, N., Weyand, E. H., Abdel-Rahman, S. M. & Sinko, P. J. An investigation of the intradermal route as an effective means of immunization for microparticulate vaccine delivery systems. *Vaccine* **18**, 2600–2612 (2000).
5. Soto, F., Mishra, R. K., Chrostowski, R., Martin, A. & Wang, J. Epidermal tattoo patch for ultrasound-based transdermal microballistic delivery. *Adv Mater Technol* **2**, 1700210 (2017).
6. Kagan, D. *et al.* Acoustic droplet vaporization and propulsion of terfluorocarbon-loaded microbullets for targeted tissue penetration and deformation. *Angewandte Chemie* **124**, 7637–7640 (2012).
7. Yildirim, A. *et al.* Nanoparticle-mediated acoustic cavitation enables high intensity focused ultrasound ablation without tissue heating. *ACS Appl Mater Interfaces* **10**, 36786–36795 (2018).
8. Kwan, J. J. *et al.* Ultrasound-propelled nanocups for drug delivery. *Small* **11**, 5305–5314 (2015).

9. Van Der Maaden, K. *et al.* Ovalbumin-coated pH-sensitive microneedle arrays effectively induce ovalbumin-specific antibody and T-cell responses in mice. *European Journal of Pharmaceutics and Biopharmaceutics* **88**, 310–315 (2014).
10. Niu, L., Chu, L. Y., Burton, S. A., Hansen, K. J. & Panyam, J. Intradermal delivery of vaccine nanoparticles using hollow microneedle array generates enhanced and balanced immune response. *Journal of Controlled Release* **294**, 268–278 (2019).
11. Du, G. *et al.* Intradermal vaccination with hollow microneedles: A comparative study of various protein antigen and adjuvant encapsulated nanoparticles. *Journal of Controlled Release* **266**, 109–118 (2017).
12. Vrdoljak, A. *et al.* Coated microneedle arrays for transcutaneous delivery of live virus vaccines. *Journal of Controlled Release* **159**, 34–42 (2012).
13. Koutsonanos, D. G. *et al.* Transdermal influenza immunization with vaccine-coated microneedle arrays. *PLoS One* **4**, e4773 (2009).
14. Stenberg, K. *et al.* Guide posts for investment in primary health care and projected resource needs in 67 low-income and middle-income countries: a modelling study. *Lancet Glob Health* **7**, e1500–e1510 (2019).
15. Sullivan, S. P. *et al.* Dissolving polymer microneedle patches for influenza vaccination. *Nat Med* **16**, 915–20 (2010).
16. Poirier, D. *et al.* Hepatitis B surface antigen incorporated in dissolvable microneedle array patch is antigenic and thermostable. *Biomaterials* **145**, 256–265 (2017).
17. Edens, C., Collins, M. L., Goodson, J. L., Rota, P. A. & Prausnitz, M. R. A microneedle patch containing measles vaccine is immunogenic in non-human primates. *Vaccine* **33**, 4712–4718 (2015).
18. Ochieng, W. O. *et al.* Uncrewed aircraft systems versus motorcycles to deliver laboratory samples in west Africa: a comparative economic study. *Lancet Glob Health* **8**, e143–e151 (2020).
19. Thio, C. L., Guo, N., Xie, C., Nelson, K. E. & Ehrhardt, S. Global elimination of mother-to-child transmission of hepatitis B: revisiting the current strategy. *The Lancet Infectious Diseases* vol. 15 981–985 Preprint at https://doi.org/10.1016/S1473-3099(15)00158-9 (2015).
20. Wang, L. *et al.* Hepatitis B vaccination of newborn infants in rural China: evaluation of a village-based, out-of-cold-chain delivery strategy. *Bull World Health Organ* **85**, 688–694 (2007).
21. Humphreys, G. Vaccination: rattling the supply chain. *Bulletin of the World Health Organization* vol. 89 324–325 Preprint at https://doi.org/10.2471/blt.11.030511 (2011).
22. Shea, B., Andersson, N. & Henry, D. Increasing the demand for childhood vaccination in developing countries: a systematic review. *BMC Int Health Hum Rights* **9**, 1–12 (2009).
23. Lee, J. W., Choi, S.-O., Felner, E. I. & Prausnitz, M. R. Dissolving microneedle patch for transdermal delivery of human growth hormone. *Small* **7**, 531–539 (2011).
24. Kim, H. K. *et al.* A comparative study of dissolving hyaluronic acid microneedles with trehalose and poly(vinyl pyrrolidone) for efficient peptide drug delivery. *Biomater Sci* **6**, 2566–2570 (2018).
25. Nguyen, H. X. *et al.* Poly (vinyl alcohol) microneedles: fabrication, characterization, and application for transdermal drug delivery of doxorubicin. *European Journal of Pharmaceutics and Biopharmaceutics* **129**, 88–103 (2018).
26. Lee, J. W., Park, J. H. & Prausnitz, M. R. Dissolving microneedles for transdermal drug delivery. *Biomaterials* **29**, 2113–2124 (2008).
27. Leone, M. *et al.* Hyaluronan-based dissolving microneedles with high antigen content for intradermal vaccination: Formulation, physicochemical characterization and immunogenicity assessment. *European Journal of Pharmaceutics and Biopharmaceutics* **134**, 49–59 (2019).
28. Lee, K., Lee, C. Y. & Jung, H. Dissolving microneedles for transdermal drug administration prepared by stepwise controlled drawing of maltose. *Biomaterials* **32**, 3134–3140 (2011).
29. Raphael, A. P. *et al.* Targeted, needle-free vaccinations in skin using multilayered, densely-packed dissolving microprojection arrays. *Small* **6**, 1785–1793 (2010).
30. Allen, E. A. *et al.* Dissolvable microneedle fabrication using piezoelectric dispensing technology. *Int J Pharm* **500**, 1–10 (2016).
31. Leone, M. *et al.* Hyaluronan-based dissolving microneedles with high antigen content for intradermal vaccination: formulation, physicochemical characterization and immunogenicity assessment. *European Journal of Pharmaceutics and Biopharmaceutics* **134**, 49–59 (2018).
32. Pei, P. *et al.* Composite-dissolving microneedle patches for chemotherapy and photothermal therapy in superficial tumor treatment. *Biomater Sci* **6**, 1414–1423 (2018).

33. Wang, Q. L. *et al.* Effect of humidity on mechanical properties of dissolving microneedles for transdermal drug delivery. *Journal of Industrial and Engineering Chemistry* **59**, 251–258 (2018).
34. Dillon, C., Hughes, H., O'Reilly, N. J. & McLoughlin, P. Formulation and characterisation of dissolving microneedles for the transdermal delivery of therapeutic peptides. *Int J Pharm* **526**, 125–136 (2017).
35. Quinn, H. L., Bonham, L., Hughes, C. M. & Donnelly, R. F. Design of a dissolving microneedle platform for transdermal delivery of a fxed-dose combination of cardiovascular drugs. *J Pharm Sci* **104**, 3490–3500 (2015).
36. Caspersen, M. B. *et al.* Thermal degradation and stability of sodium hyaluronate in solid state. *Carbohydr Polym* **107**, 25–30 (2014).
37. Leone, M. *et al.* Universal applicator for digitally-controlled pressing force and impact velocity insertion of microneedles into skin. *Pharmaceutics* **10**, (2018).
38. Chen, H. *et al.* A novel scalable fabrication process for the production of dissolving microneedle arrays. *Drug Deliv Transl Res* **9**, 240–248 (2019).
39. Pere, C. P. P. *et al.* 3D printed microneedles for insulin skin delivery. *Int J Pharm* **544**, 425–432 (2018).
40. McGrath, M. G. *et al.* Production of dissolvable microneedles using an atomised spray process: Effect of microneedle composition on skin penetration. *European Journal of Pharmaceutics and Biopharmaceutics* **86**, 200–211 (2014).
41. O'Mahony, C. *et al.* Accuracy and feasibility of piezoelectric inkjet coating technology for applications in microneedle-based transdermal delivery. *Microelectron Eng* **172**, 19–25 (2017).
42. Römgens, A. M., Bader, D. L., Bouwstra, J. A. & Oomens, C. W. J. Predicting the optimal geometry of microneedles and their array for dermal vaccination using a computational model. *Comput Methods Biomech Biomed Engin* **19**, 1599–1609 (2016).
43. Schift, H. *et al.* Fabrication of polymer photonic crystals using nanoimprint lithography. in *Nanotechnology* vol. 16 S261 (IOP Publishing, 2005).
44. Worgull, M., Kabanemi, K. K., Marcotte, J. P., Hétu, J. F. & Heckele, M. Modeling of large area hot embossing. in *Microsystem Technologies* vol. 14 1061–1066 (Springer, 2008).
45. Lee, I. C., Wu, Y. C., Tsai, S. W., Chen, C. H. & Wu, M. H. Fabrication of two-layer dissolving polyvinylpyrrolidone microneedles with different molecular weights for: In vivo insulin transdermal delivery. *RSC Adv* **7**, 5067–5075 (2017).
46. Fukushima, K. *et al.* Two-layered dissolving microneedles for percutaneous delivery of peptide/protein drugs in rats. *Pharm Res* **28**, 7–21 (2011).
47. Chu, L. Y. *et al.* Enhanced Stability of Inactivated Influenza Vaccine Encapsulated in Dissolving Microneedle Patches. *Pharm Res* **33**, 868–878 (2016).
48. Pan, J. *et al.* Intradermal delivery of STAT3 siRNA to treat melanoma via dissolving microneedles. *Sci Rep* **8**, (2018).

SUPPLEMENTARY INFORMATION

Table S1. The concentration of polymer formulation for polymer screening and the results of dMNA fabrication. Only successful formulations were used for further studies.

Polymer	Concentration (w/v) (%)	Fabrication	Failed reason
PVP/PEG	52	succeeded	
	26	succeeded	
	13	succeeded	
	6.5	succeeded	
	3.25	failed	brittle
PVA	50	failed	too viscous
	40	succeeded	
	30	succeeded	
	20	succeeded	
	10	succeeded	
	5	succeeded	
5 kDa HA	10	failed	brittle
10 kDa HA	10	succeeded	
20 kDa HA	10	succeeded	
100 kDa HA	10	succeeded	
Gelatin	40	succeeded	
CMC	30	failed	too viscous
	20	succeeded	
	10	succeeded	

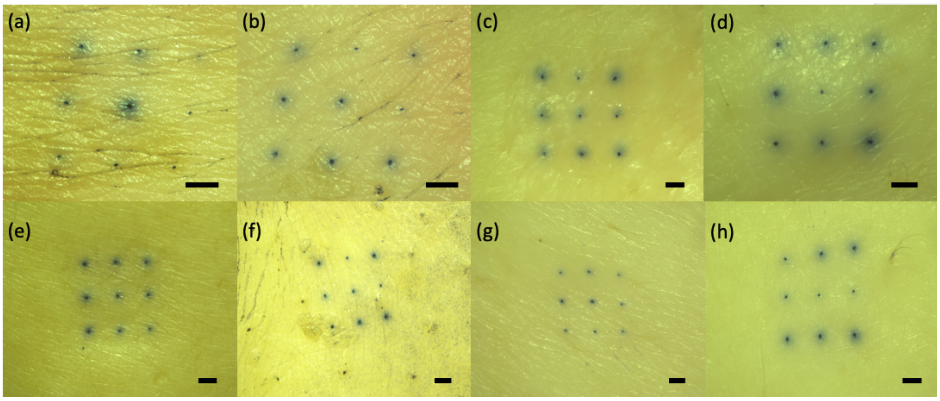

Figure S1. Ex vivo human skin penetration test. Representative examples of penetrated ex vivo human skin with 10% (w/v) HA 10 kDa (a), 10% (w/v) HA 20 kDa (b), 6.5% (w/v) PVP/PEG (c), 26% (w/v) PVP/PEG (d), 5% (w/v) PVA (e), 20% (w/v) PVA (f), 10% (w/v) CMC (g), 40% (w/v) gelatin (h) dMNA. (All scale bar = 1 mm).

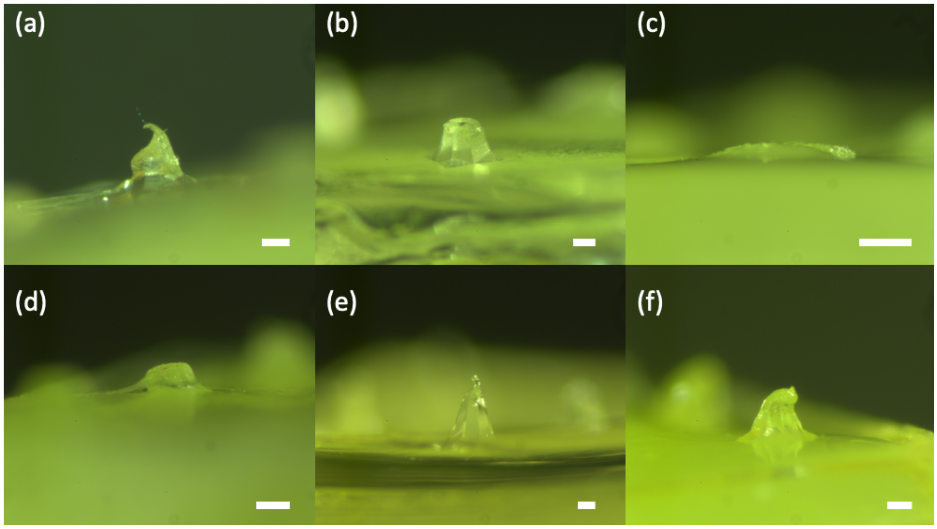

Figure S2. Remained microneedles after 5 min of dissolution. 10% (w/v) HA 10 kDa (a), 10% (w/v) HA 20 kDa (b), 6.5% (w/v) PVP/PEG (c), 5% (w/v) PVA (d), 10% (w/v) CMC (e), 40% (w/v) Gelatin (f). The dissolution test was performed on the ex vivo human skin at RT. (All scale bar = 100 µm).